JOURNAL OF PROPULSION AND POWER
Vol. 26, No. 4, July–August 2010

Semi-Empirical Model for Reaction Progress in Nanothermite

Adam Trebs* and Timothy J. Foley†
Los Alamos National Laboratory, Los Alamos, New Mexico 87545

DOI: 10.2514/1.46607

Calculations of thermite reaction progress were made using the Cheetah thermochemistry package. Progress was modeled by fractionally substituting reactants with an inert species with identical thermodynamic properties. The results of this model have been used to create a semi-empirical model of regression rate. The acceptability of the D^2 particle regression law for nanothermite systems of a scale on the order of 10 nm has been demonstrated. Additionally a strong sensitivity to composition is demonstrated.

Nomenclature

D	=	diameter of particle assumed to be spherical
n	=	spatial exponent in regression law
t	=	time
x	=	characteristic dimension
Y	=	mass fraction
β	=	time coefficient for particle regression

Subscripts

Al	=	total Al content
Al-inert	=	only the inert fraction
p	=	at pressure peak
0	=	initial condition or arrival time

I. Introduction

AS PARTICLE sizes approach tens of nanometers in thermites, propagation velocities can be on the order of thousands of meters/second [1,2]. Additionally, as reaction propagates in these materials, a significant pressure pulse is developed locally (∼100 atm). The scale of reaction is small enough that the reaction proceeds at a rate that allows a nearly constant-volume adiabatic process [3]. As a result of this localized high-pressure hot products are propelled away from the reaction zone leading to a convective propagation [1]. Further, the Biot number associated with the particles in this environment is very small, so they approach quasi-thermal equilibrium. Malchi et al. [3] demonstrated the ability to model peak pressures of nanothermite reactions based entirely on equilibrium thermochemistry under the assumption of constant-volume adiabatic combustion.

Recent work on the combustion of aluminum describes a novel transport mechanism within the oxidation process [4,5]. Called the melt-dispersion mechanism (MDM), this process is the dispersion of a molten aluminum core by cavitation in a rarefaction wave that results from the bursting of the alumina mantle by expansion of the aluminum core upon melting. This creates a cloud of aluminum droplets that oxidizes on a scale limited by kinetics.

The goal of the current work is to expand upon the work of Malchi et al. [3] by attempting to model reaction progress under a quasi-equilibrium assumption. For this study aluminum is used as the limiting reagent to simulate progress, but the result is the same as using the oxide as the limiting reagent. The calculated progress is fit to experimental data in an attempt to describe a regression law that can yield insights into reaction mechanisms.

The goal of the regression law here is to relate the physical size of the particle to reaction progress. The classical particle model with closed analytical solution is the D^2 law:

$$D^2 = D_0^2 - \beta t \tag{1}$$

This solution assumes that reaction progress is diffusion-dominated, and the closed form values of β also additionally assume a single particle in a quiescent environment. For cases in which the reaction is not diffusion-dominated the exponent is reduced. For a particle in a laminar convective flow the exponent approaches 1.5, and for turbulent convection or a kinetically dominated condition the exponent approaches 1.0 [6,7].

II. Calculation

The Cheetah [8] thermochemistry package was used to simulate nanoaluminum/copper-oxide, nanoaluminum/molybdenum-oxide, nanoaluminum/tungsten-oxide, and nanoaluminum/bismuth-oxide thermites. These materials were chosen for this study because of the availability of data from a previous study [9]. Pressure traces from burn-tube experiments are the data to which the calculations were compared. The pressure-history data were taken at several axial points along a 3.2-mm-i.d., 88.9-mm-long tube. The tubes were loaded by pouring the thermite into the tube and vibrating with a Cleveland vibrating block. A full description of these experiments is available elsewhere [9]. The simulation was performed with the constant-volume combustion routine using a modified JCZS library‡; it has been shown to effectively predict peak pressure for rapidly propagating nanothermites [3].

Reaction progress was simulated by limiting the amount of aluminum that participates in the reaction. The nonparticipating fraction of aluminum was replaced by an inert species with identical thermodynamic properties to that of aluminum. In this way progress could be modeled though discrete levels of aluminum consumption. The equilibrium composition, temperature, and pressure were calculated at 11 evenly spaced nonparticipating aluminum to total aluminum mass ratios from 1 to 0 inclusive. This assumes quasi-equilibrium throughout the reaction and a mechanical reaction limitation.

The composition of the thermite pack to be analyzed was calculated from the data available in [9]. The density was taken as the density of the solids, and the mass of interstitial air was added to the mass of the solid fraction. The given equivalence ratios were used to calculate the mass fractions assuming a simple single replacement reaction and an 88% active aluminum content for the nano-aluminum. For copper-oxide, molybdenum-oxide, tungsten-oxide,

Received 3 August 2009; revision received 11 February 2010; accepted for publication 8 March 2010.

*Graduate Student, Dynamic and Energetic Materials, Explosive Applications and Special Projects. Student Member AIAA.

†Program Manager, Dynamic and Energetic Materials, Explosive Applications and Special Projects.

‡Baer, M. R., Private Communication, 2006.

and bismuth-oxide the densities of the solid pack were 0.311, 0.498, 0.522, and 1.24 g/cm^3, and the equivalence ratios were 1, 1.4, 1.8, and 1.3. The equivalence ratio here is taken as the mass ratio of atomic aluminum to transition metal oxide in the experiment divided by that ratio at stoichiometric conditions. Small amounts of water, on the order of 1% by mass, were added to the composition for some calculations; this water was taken as part of the transition metal-oxide mass fraction.

Following calculations of reaction progress based upon the percentage of aluminum consumed, the spatial progression was related to the temporal progression by fitting the calculated pressure pulse to the experimental pressure pulse. The geometry of the problem is shown in Fig. 1. Assuming spatial regression takes a power law form, like the D^2 law, the spatial progress relates to aluminum consumption as follows:

$$\frac{x}{x_0} = \left[\frac{Y_{\text{Al-inert}}}{Y_{\text{Al}}}\right]^{\frac{1}{3}}$$

$$t - t_0 = \frac{x_0^n - x^n}{\beta} = \frac{x_0^n}{\beta}\left(1 - \left[\frac{x}{x_0}\right]^n\right) = \frac{x_0^n}{\beta}\left(1 - \left[\frac{Y_{\text{Al-inert}}}{Y_{\text{Al}}}\right]^{\frac{n}{3}}\right)$$

$$\Rightarrow t = t_0 + \left[1 - \left[\frac{Y_{\text{Al-inert}}}{Y_{Al}}\right]^{\frac{n}{3}}\right](t_p - t_0) \qquad (2)$$

The values n, t_p and t_0 are fitting parameters. The numbers assigned to t_p and t_0 are taken directly from experimental data; they are the end and beginning of pressure response. The exponent n is the interesting value in this problem. It relates burn time to the dimensions of the problem (e.g., the classic D^2 law for droplet regression) and is determined by the mechanics of regression as described above. As the calculated pressure, temperature, and chemical data are at discrete ratios of participating aluminum to total aluminum content, this equation allows the relation of the calculated information to time.

The pressure histories that were used for fitting were averaged versions of fully developed traces. The fully developed traces are the most repeatable and demonstrated the constant-volume behavior. The averaging was accomplished by adjusting trace magnitude so the initial pressure is 0.8 atm (the local pressure) and modulating the temporal dimension so all the times of arrival, t_0 coincided. For any given thermite mixture, there was a high variability in the experimental pressure data that could not be explained outside of variation in composition: moisture, oxidation, pretest reaction. As a consequence, some data were not used for fitting.

III. Results

The pressure traces calculated for the copper-oxide, molybdenum-oxide, and tungsten-oxide systems were readily fit to the averaged experimental traces. The experimental and calculated pressure traces for these materials are shown in Fig. 2. The exponent in the calculated time for all three systems is 2. This was the best fit that could be achieved, and was significantly better than lower values: 1 and 1.5. In the following total action time is taken from the fits of the calculations. Total action time is the value of t_p-t_0 used that gives an appropriate fit and is the time from the beginning of the reaction to the fitted end of reaction based upon the calculated chemistry.

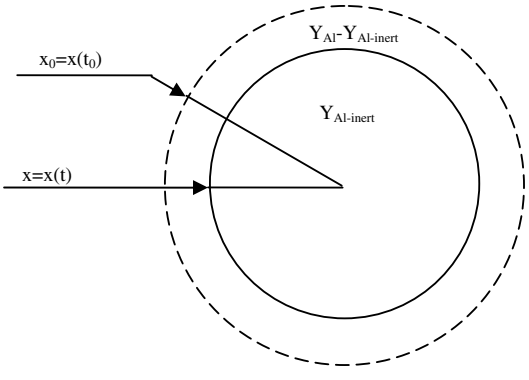

Fig. 1 Theoretical geometry of the problem.

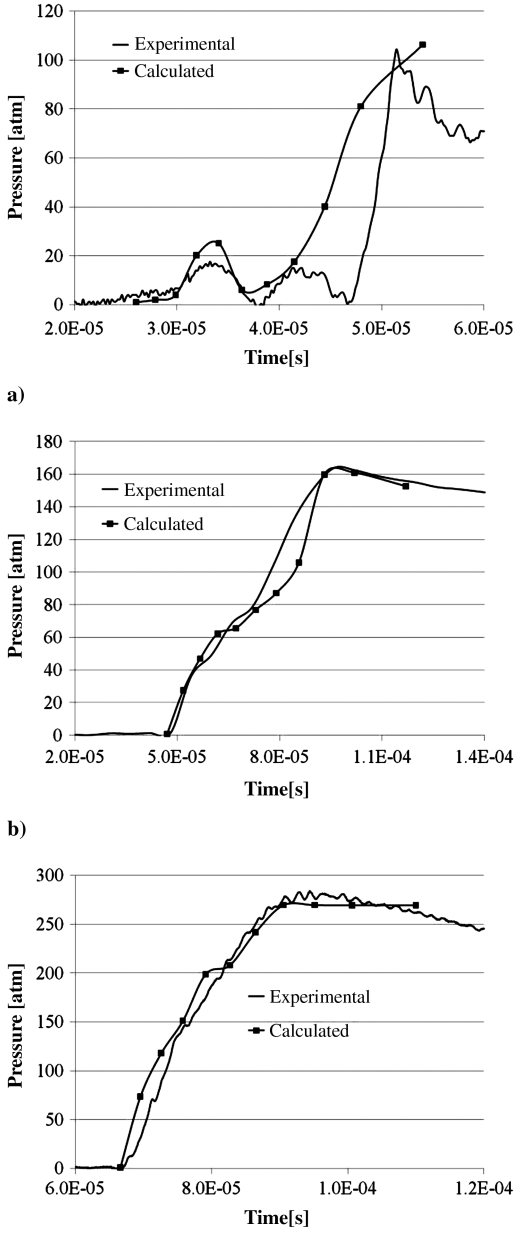

Fig. 2 Experimental data and semi-empirical model for a) nAl/CuO(.311 g/cm^3), b) nAl/MoO_3(.498 g/cm^3), and c) nAl/WO_3(.522 g/cm^3).

The total action time for the copper-oxide system was 28 μs. There are some interesting features in the pressure history for this system. There are two minor pressure maxima before the primary maximum. The first maximum is related to the progress of the reaction. It is expected that the minimum following the second local maximum in the copper-oxide system pressure trace is nonphysical and is the result of a structural response or vibration on the transducer or confinement, because in unaveraged traces, the minimum was frequently negative on an absolute scale. Also, the primary maximum tended to fit better to individual histories than the averaged because of variability in the time between the first maxima and the primary maxima. It is possible that before the primary maximum that the process is not occurring at a constant volume as a result of the shallower gradient. This may explain both the low pressure of the first maximum in comparison to the calculated and the variability in the time between the extrema.

The molybdenum-oxide system pressure history does not have nearly as much structure as the copper-oxide system pressure history. The total action time of the molybdenum-oxide system is 70 μs. The deviation between the experimental and calculated trace coincides with the calculated melt of the molybdenum; this deviation may be the result of the kinetics of melt in the actual system. The molybdenum-oxide system calculations assumed the oxide was 1.5% H_2. by mass. This accounts for water present in the actual oxide and generates the required pressure output. In the absence of water the pressure output is 73 atm. This also illustrates the sensitivity of this reaction to the presence of water: 1.5% water in the composition more than doubles the pressure output.

The fit of the tungsten-oxide system pressure history is better than either of the previous two. The total action time of the tungsten-oxide system is 43 μs. There are two major calculated features that deviate from the experimental trace. There is a step that appears in the calculated trace at approximately 80 μs that does not appear in the experimental trace. This step corresponds to some odd behavior in the tungsten-oxide species; this will be discussed later. Also, the calculated trace attains a constant pressure. This does not occur in the experimental trace because of venting of the tube. Tungsten-oxide with 4.2% H_2 by mass generates a calculated peak pressure matching the experimental peak, so this moisture content is used for the calculations. Tungsten-oxide readily forms crystalline hydrates; a sample composed entirely of the monohydrate would have a 7.2% water content. Additionally, surface moisture can exist on all the materials of the thermite. This system has similarly extreme moisture sensitivity to the molybdenum-oxide system.

The composition and temperature histories for the copper-oxide, molybdenum-oxide, and tungsten-oxide systems are shown in Fig. 3. They are simply shown against reaction progress as there is no experimental data to which to compare; this does give the curves an appropriate temporal shape. These traces only show dominant gas-phase species. These are the most pertinent to shape of the pressure history and of more interest than the condensed phase. Throughout the reaction the mass fractions of species in the condensed phases are two orders of magnitude greater than the gas phase.

The copper-oxide system shows a distinct peak in gas-phase oxygen content that corresponds to a thermal reduction of CuO to Cu_2O; this peak also corresponds to the first maximum in the pressure history. After this initial maximum, the next pressure peak is driven by increasing temperature in conjunction with a growing gas phase, dominated by Cu(g) and aluminum species.

The molybdenum-oxide system shows a trough in total gas content mid burn combined with a monotonic increase in temperature. The minimum in gas content coincides with the shallow section of pressure history. The lower section of the composition history is dominated by water and molybdic acid. The upper section of the composition history is dominated by monoatomic hydrogen and aluminum species. The decrease in pressure at the end of the calculated history is the result of the consumption of a portion of the aluminum gas phase. Physically, this chemical effect is superimposed over the mechanical effect of the venting of the tube.

The tungsten-oxide system shows some odd chemical behavior in both the gas and condensed phases. In the condensed phase there is a local minimum in tungsten (VI) oxide that relates to both a peak in tungsten (IV) oxide in the condensed phase and to the peak in tungstenic acid in the gas phase. This all corresponds to steps in the pressure and temperature that appear to be nonphysical. It is possible that the kinetics of the conversion to tungstenic acid are slow enough as to make this step less prominent in these reactions. It is also possible that there is a flaw in the calculations in this range: the apparent conversion from tungsten (IV) oxide back to tungsten (VI) oxide (which is less dense) with increasing temperature and pressure is odd. It is also interesting that the rate of propagation of this reaction is greatest at an equivalence ratio of 1.8 but aluminum is never a major species in the gas phase.

This method of calculation appears to be less effective for modeling the bismuth-oxide system. Figure 4 shows several sets of calculated data with experimental data for the bismuth-oxide system.

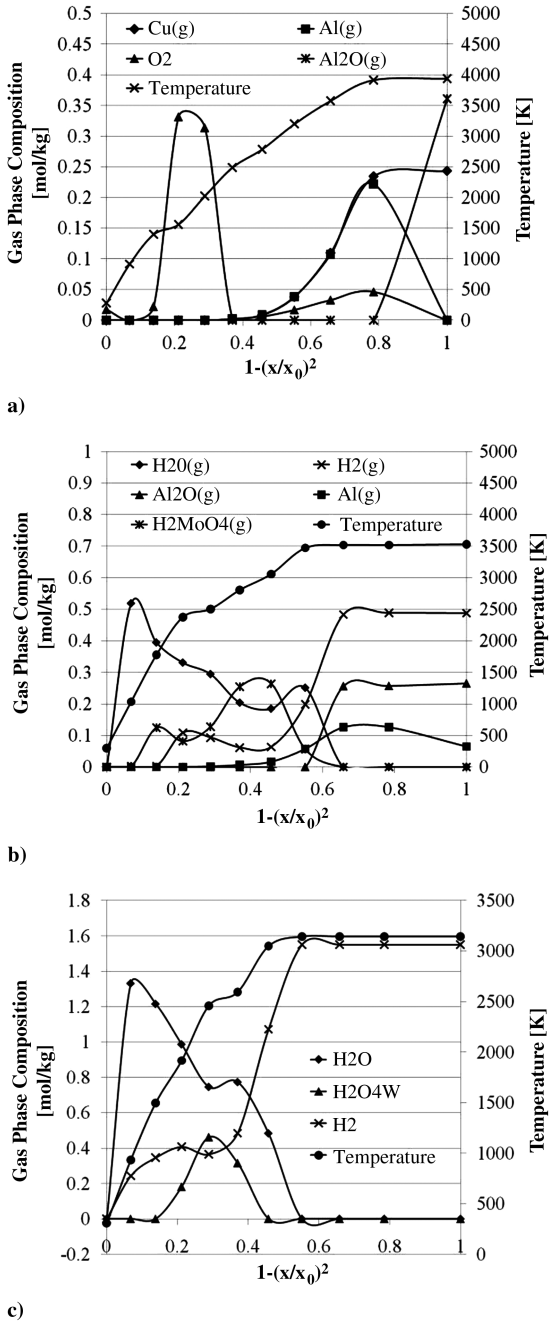

Fig. 3 Calculated gas-phase composition and temperature for a) nAl/CuO, b) nAl/MoO_3, and c) nAl/WO_3.

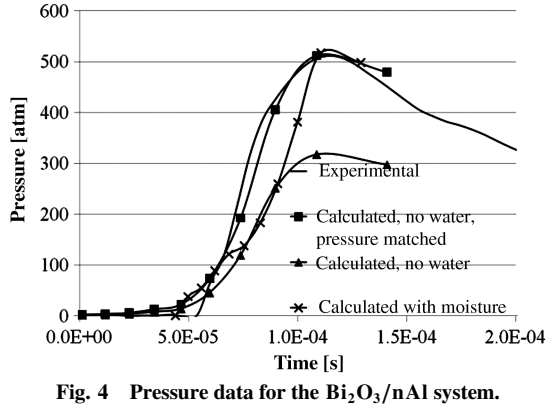

Fig. 4 Pressure data for the Bi_2O_3/nAl system.

In the absence of moisture the calculated peak pressure for this system is approximately 60% of the experimental peak, but this result by itself is not unexpected. Though, when enough water is added to the calculated system to match peak pressure, the calculated pressure history can no longer be effectively fit to experimental data even by changing the exponent, n. On the other hand, the shape of the curve in the absence of water closely matches the experimental curve; when the calculated pressure peak is amplified to match the experimental peak, the two histories match well. It is possible the bismuth chemistry used here is not very well refined[§]; there are no published examples of calculations of bismuth chemistry with Cheetah. The steps in the data from the calculations that include moisture correspond to vaporization and reduction of the water.

IV. Conclusions

It was demonstrated through the above described calculations that nanothermite reactions are very sensitive to moisture content. The pressure pulse of these reactions is the result of a very small gas phase; as a consequence, the addition of a small amount of water can lead to a significant addition to the gas phase. Further, when aluminum reacts with water the H and H_2 that is released adds greater molar content to the gas phase than the initial moisture. Finally, by mass, water yields a greater energy output than molybdenum-trioxide when reacted with aluminum.

Upon initial examination of the experimental data from the copper-oxide system, it might be easy to discount the initial pressure pulse as nonphysical. Using the above calculations, this pressure pulse was replicated from thermochemistry. Minima in gas-phase content versus time are physical and measurable.

In this study it was assumed that the rate of regression or consumption of the material related to the dimension of the particulate to some power. It was found, based on fitting calculated reaction progress to experimental data that under these particular conditions nanothermites appear to obey a D^2 regression law. While classic derivations of the D^2 law assume single particles in a quiescent environment, this type of scaling appears to be applicable to these confined particle packs with convection and high speed reaction. Perhaps this is the result of the system being dominated by condensed phases.

Based on the accuracy of the above calculation both in terms of peak pressure and pressure trace shape, it is suggested that these systems are mechanically limited. The reaction progress follows a D^2 law, which is indicative of diffusion-controlled reaction, and the exponent is larger than one would expect for other control mechanisms. Because of the accuracy of these calculations, which assume quasi-equilibrium, a transport-dominated rate mechanism is more likely than a kinetic mechanism, and the high pressure is not the result of an intermediate gas phase. In light of the MDM for aluminum combustion, it is likely that the regression mechanics and reaction progress of these systems are dominated by the behavior of the transition metal-oxide phase.

References

[1] Asay, B. W., Son, S. F., Busse, J. R., and Oschwald, D. M., "Ignition Characteristics of Metastable Intermolecular Composites," *Propellants, Explosives, Pyrotechnics*, Vol. 29, No. 4, 2004, pp. 216–219. doi:10.1002/prep.200400049

[2] Bockmon, B. S., Pantoya, M. L., Son, S. F., Asay, B. W., and Mang, J. T., "Combustion Velocities and Propagation Mechanism of Metastable Interstitial Composites," *Journal of Applied Physics*, Vol. 98, 2005, Paper 064903. doi:10.1063/1.2058175

[3] Malchi, J. Y., Yetter, R. A., Foley, T. J., and Son, S. F., "The Effect of Added Al_2O_3 on the Propagation Behavior of an Al/CuO Nanoscale Thermite," *Combustion Science and Technology*, Vol. 180, 2008, pp. 1278–1294. doi:10.1080/00102200802049471

[4] Levitas, V. I., Pantoya, M., and Dikici, B., "Melt Dispersion Versus Diffusive Oxidation Mechanism for Aluminum Nanoparticles: Critical Experiments and Controlling Parameters," *Applied Physics Letters*, Vol. 92, 2008, p. 011921. doi:10.1063/1.2824392

[5] Levitas, V. I., "Burn Time of Aluminum Nanoparticles: Strong Effect of the Heating Rate and Melt-Dispersion Mechanism," *Combustion and Flame*, Vol. 156, 2009, pp. 543–546. doi:10.1016/j.combustflame.2008.11.006

[6] Glassman, I., *Combustion*, 3rd ed., Academic Press, San Diego, CA, 1996, Chap. 6.

[7] King, M. K., "Ignition and Combustion of Boron Particles and Clouds," *Journal of Spacecraft and Rockets*, Vol. 19, No. 4, 1982, pp. 294–306. doi:10.2514/3.62256

[8] Cheetah, Software Package, Ver. 5.0, Lawrence Livermore National Lab., Livermore, CA, 2007.

[9] Sanders, V. E., Asay, B. W., Foley, T. J., Tappan, B. C., Pacheco, A. N., and Son, S. F., "Reaction Propagation of Four Nanoscale Energetic Composites (Al/MoO_3, Al/WO_3, Al/CuO, and Bi_2O_3)," *Journal of Propulsion and Power*, Vol. 23, No. 4, 2007, pp. 707–714. doi:10.2514/1.26089

S. Son
Associate Editor

[§]Private communication with S. Bastea, 2009.